A combined ADER-DG and PML approach for simulating wave propagation in unbounded domains

Thomas G. Amler, Ibrahim Hoteit, and Tariq A. Alkhalifah

Citation: AIP Conference Proceedings **1479**, 1251 (2012); doi: 10.1063/1.4756380
View online: http://dx.doi.org/10.1063/1.4756380
View Table of Contents: http://scitation.aip.org/content/aip/proceeding/aipcp/1479?ver=pdfcov
Published by the AIP Publishing

A Combined ADER-DG and PML Approach for Simulating Wave Propagation in Unbounded Domains

Thomas G. Amler, Ibrahim Hoteit and Tariq A. Alkhalifah

King Abdullah University of Science and Technology (KAUST), MCSE, Thuwal 23955-6900. Saudi Arabia

Abstract. In this work, we present a numerical approach for simulating wave propagation in unbounded domains which combines discontinuous Galerkin methods with arbitrary high order time integration (ADER-DG) and a stabilized modification of perfectly matched layers (PML). Here, the ADER-DG method is applied to Bérenger's formulation of PML. The instabilities caused by the original PML formulation are treated by a fractional step method that allows to monitor whether waves are damped in PML region. In grid cells where waves are amplified by the PML, the contribution of damping terms is neglected and auxiliary variables are reset. Results of 2D simulations in acoustic media with constant and discontinuous material parameters are presented to illustrate the performance of the method.

Keywords: discontinuous Galerkin method, arbitrary high order, perfectly matched layer, stabilization.
PACS: 02.70.Dh, 91.30.Ab.

INTRODUCTION

In many problems involving wave propagation, the spatial domain in which waves can propagate is much larger than the domain where the wave field is of interest. For example, when seismic surveys are used for reservoir monitoring, seismic waves do not only propagate through the reservoir but through a much larger region in the subsurface. A major challenge in simulating such phenomena is the determination of non-reflecting boundary conditions (NRBC) so that the computational domain can be truncated without perturbing the computed wave field in the domain of interest. Since exact NRBC are often non-local in time and space (see e.g. [1, 2]), absorbing layers are frequently used to treat artificial boundaries. Here, we present a numerical scheme that combines discontinuous Galerkin methods with arbitrary high order time integration (ADER-DG) and a stabilized modification of perfectly matched layers (PML). Since instabilities can be observed if the original formulation is used to truncate the computational domain (see e.g. [3, 4, 5, 6]), we use a fractional step method that enables monitoring whether waves are damped in the PML region.

FORMULATION OF GOVERNING EQUATIONS

Wave propagation in 2D acoustic (or elastic) media can be described by a system of first order PDEs of the form

$$\partial_t q + A_x \partial_x q + A_y \partial_y q = 0 \tag{1}$$

where q is the unknown $\mathbb{R}^m$-valued function, and A_x and A_y are space dependent Jacobian matrices. For the presentation here, we assume that no external sources are present. The number m, of unknown functions in Eq. (1) depends on the considered physical model. For example, in the case of isotropic acoustic media, we have $m = 3$ and

$$q = \begin{bmatrix} p \\ u \\ v \end{bmatrix}, \qquad A_x = \begin{bmatrix} 0 & E & 0 \\ 1/\rho & 0 & 0 \\ 0 & 0 & 0 \end{bmatrix}, \qquad \text{and} \qquad A_y = \begin{bmatrix} 0 & 0 & E \\ 0 & 0 & 0 \\ 1/\rho & 0 & 0 \end{bmatrix} \tag{2}$$

where p denotes pressure, u and v particle velocities in x and y direction, resp., E the P-wave modulus, and ρ density (see [7]). In the case of elastic media, p is replaced by components of the stress tensor τ, i.e. $q = [\tau_{11}, \tau_{22}, \tau_{12}, u, v]^T$, $m = 5$, and A_x and A_y depend on density and Lamé parameters (see [8]).

System (1) is considered on the whole space $\mathbb{R}^2$ but numerical solutions will have to be computed on a bounded domain $\tilde{\Omega} \subset \mathbb{R}^2$. To this end, the domain of interest, denoted by Ω, is surrounded by absorbing layers, the PML region, in such a way that no reflections are generated at the interface between Ω and the PML region. In Bérenger's

Numerical Analysis and Applied Mathematics ICNAAM 2012
AIP Conf. Proc. 1479, 1251-1254 (2012); doi: 10.1063/1.4756380

formulation, the unknown vector function q is split into two components, q^1 and q^2, such that $q^1+q^2=q$, and system (1) is split according to the spatial derivatives. The resulting PML formulation of system (1) is given by

$$\partial_t q^1 + A_x\,\partial_x\left(q^1+q^2\right)+\sigma_1\,q^1=0, \qquad \partial_t q^2 + A_y\,\partial_y\left(q^1+q^2\right)+\sigma_2\,q^2=0 \tag{3}$$

where σ_1 and σ_2 are non-negative damping functions that vanish in Ω [5, 3].

It has been reported in the literature that blow up phenomena or long time instabilities can be observed when Eqs. (3) are used to truncate the computational domain [3, 4, 5, 6]. To overcome this difficulty, the following modification has been introduced and analyzed in [3]. System (3) is written in terms of unknowns q and $\tilde{q}:=q_1$:

$$\partial_t q + A_x\,\partial_x q + A_y\,\partial_y q + \sigma_2\,q + (\sigma_1-\sigma_2)\,\tilde{q}=0, \qquad \partial_t \tilde{q} + A_x\,\partial_x q + \sigma_1\,\tilde{q}=0. \tag{4}$$

Further, the damping term $(\sigma_1-\sigma_2)\tilde{q}$ in system (4) is regularized

$$\partial_t q + A_x\,\partial_x q + A_y\,\partial_y q + \sigma_2\,q + (\sigma_1-\sigma_2)\,\psi_\varepsilon * \tilde{q}=0, \qquad \partial_t \tilde{q} + A_x\,\partial_x q + \sigma_1\,\tilde{q}=0 \tag{5}$$

where ψ_ε is a smooth function which approximates the Dirac measure. A well-posedness result for the Cauchy problem of Eqs. (5) is shown in the cases of linearized Euler equations and Maxwell's equations.

In the next section, we will also consider Eqs. (4) but use a different modification that is easier to implement in high order finite element frameworks than Eqs. (5). The main idea is to apply the zero order terms only in those grid cells where the sum $\sigma_2\,q+(\sigma_1-\sigma_2)\tilde{q}$ yields damping of the physical wave field q.

THE NUMERICAL SCHEME

We solve system (4) by operator splitting to be able to monitor whether the zero order terms damp or amplify the physical part, q, of the solution. To describe our approach, we first fix the notation. Assume that the computational domain, $\tilde{\Omega}$, is divided into K straight-sided conforming triangular elements, $\tilde{\Omega}\simeq\tilde{\Omega}_h=\bigcup_{k=1}^{K}\mathsf{D}^k$ and A_x, A_y, σ_1, and σ_2 are constant inside each triangle. Let $\mathsf{D}_R=\{(\xi,\eta)\,:\,\xi,\eta\geq -1;\ \xi+\eta\leq 0\}$ be a reference triangle and $\mathbb{P}_N(\mathsf{D}_R)=\text{span}\{\xi^i\eta^j\,:\,i+j\leq N;\ (\xi,\eta)\in\mathsf{D}_R\}$ the space of polynomials of degree less or equal to N [9, 10]. If q and $\tilde{q}$ are m-vector functions, let $\{\phi^j\,:\,j=1,\ldots,N_p\}$ be an orthonormal basis of $(\mathbb{P}_N(\mathsf{D}_R))^m$ with respect to the $(L^2(\mathsf{D}_R))^m$-inner product: $\int_{\mathsf{D}_R}\sum_{l=1}^{m}\phi_l^i\phi_l^j=\delta_{ij}$. Inside each element D^k, q and $\tilde{q}$ are approximated by q_h and $\tilde{q}_h$ which are defined by

$$q_h(x,y,t)=\sum_{j=1}^{N_p}q_j^k(t)\,\phi^j(\xi,\eta) \qquad \text{and} \qquad \tilde{q}_h(x,y,t)=\sum_{j=1}^{N_p}\tilde{q}_j^k(t)\,\phi^j(\xi,\eta) \qquad \Big((x,y)\in\mathsf{D}^k\Big)$$

where ξ and η are coordinates in the reference element D_R corresponding to coordinates x and y in element D^k. Set $q^n=q_h(\cdot,\cdot,t^n)$ and $\tilde{q}^n=\tilde{q}_h(\cdot,\cdot,t^n)$ where t^n are the time levels at which q_h and $\tilde{q}_h$ are computed. We first describe the general approach for computing q^{n+1} and $\tilde{q}^{n+1}$ at the next time level; boundary conditions and details of the implementation are given later. q^{n+1} and $\tilde{q}^{n+1}$ are computed in three steps:

1. Compute intermediate solutions $q^{n+1/3}$ and $\tilde{q}^{n+1/3}$ at $t=t^{n+1}$ by solving

$$\partial_t q + A_x\,\partial_x q + A_y\,\partial_y q=0, \quad q(t^n)=q^n, \qquad \text{and} \qquad \partial_t\tilde{q}+A_x\,\partial_x q=0, \quad \tilde{q}(t_n)=\tilde{q}^n. \tag{6}$$

2. Compute $q^{n+2/3}$ and $\tilde{q}^{n+2/3}$ at $t=t^{n+1}$ by solving

$$\partial_t q+\sigma_2\,q=(\sigma_2-\sigma_1)\,\tilde{q}, \quad q(t^n)=q^{n+1/3}, \qquad \text{and} \qquad \partial_t\tilde{q}+\sigma_1\,\tilde{q}=0, \quad \tilde{q}(t_n)=\tilde{q}^{n+1/3}. \tag{7}$$

3. Compute q^{n+1} and $\tilde{q}^{n+1}$ in each grid cell D^k of the PML region, $\tilde{\Omega}\setminus\Omega$, by the following distinction of cases

$$\begin{cases} q^{n+1}|_{\mathsf{D}^k}:=q^{n+2/3}, \quad \tilde{q}^{n+1}|_{\mathsf{D}^k}:=\tilde{q}^{n+2/3} & \text{if } \|q^{n+2/3}\|_{L^2(\mathsf{D}^k)}\leq\|q^{n+1/3}\|_{L^2(\mathsf{D}^k)}, \\ q^{n+1}|_{\mathsf{D}^k}:=q^{n+1/3}, \quad \tilde{q}^{n+1}|_{\mathsf{D}^k}:=sgn(\sigma_1-\sigma_2)\,q^{n+1/3}, & \text{if } \|q^{n+2/3}\|_{L^2(\mathsf{D}^k)}>\|q^{n+1/3}\|_{L^2(\mathsf{D}^k)} \end{cases} \tag{8}$$

where *sgn* denotes the sign function.

That is, the unknowns are first advanced in time without the zero order terms and then the contribution of zero order terms is computed. If this contribution causes amplification of q, it is neglected and $\tilde{q}$ is reset such that damping can be expected in the next time step. This scheme is only first order accurate in time, however, notice that the operator splitting influences q only in the PML region because $\sigma_1 = \sigma_2 = 0$ in Ω. Next, the implementation of the steps above is described.

Step 1: We use the ADER-DG technique [8, 11] to solve Eqs. (6). To this end, an expression for higher order time derivatives of q can be obtained by appling the Cauchy-Kowaleski scheme to the first equation in Eqs. (6). It holds $\partial_t^j q = [-A_x\,\partial_x - A_y\,\partial_y]^j q$ where the right-hand side means that the differential operator $-A_x\,\partial_x - A_y\,\partial_y$ is j times applied to the function q, e.g., $[-A_x\,\partial_x - A_y\,\partial_y]^2 q = A_x^2\,\partial_x^2 q + (A_x A_y + A_y A_x)\partial_x\partial_y q + A_y^2\,\partial_y^2 q$. Thus, an N^{th}-order in time approximation of q is given by

$$q(x,y,t^n+\tau) \approx \sum_{j=0}^{N} \frac{\tau^j}{j!}\,\partial_t^j q(x,y,t^n) = \sum_{j=0}^{N} \frac{\tau^j}{j!}\,[-A_x\,\partial_x - A_y\,\partial_y]^j\, q(x,y,t^n) \qquad (\tau \in \mathbb{R})\,. \tag{9}$$

Relation (9) can be used to derive weak forms of Eqs. (6). A weak form of the first system of PDEs in (6) is given by

$$\begin{aligned}\int_{\mathsf{D}^k} \phi^i \cdot q^{n+1/2} = \int_{\mathsf{D}^k} \phi^i \cdot q^n + \sum_{j=0}^{N} \frac{\Delta t^{j+1}}{(j+1)!} \int_{\mathsf{D}^k} \left[(\partial_x \phi^i)^T A_x + (\partial_y \phi^i_y)^T A_y\right] [-A_x\,\partial_x - A_y\,\partial_y]^j\, q^n \\ - \sum_{l=1}^{3}\sum_{j=0}^{N} \frac{\Delta t^{j+1}}{(j+1)!} \int_{e_l} \phi^i \cdot \left(M_l^+ \,[-A_x\,\partial_x - A_y\,\partial_y]^j\, q^{n,k} + M_l^- \left[-A_x^{k_l}\,\partial_x - A_y^{k_l}\,\partial_y\right]^j q^{n,k_l}\right)\end{aligned} \tag{10}$$

for $i = 1,\ldots,N_p$. In Eq. (10), e_l denotes an edge of D^k, D^{k_l} the corresponding neighbor element, $q^{n,k}$ and q^{n,k_l} the traces of q^n on e_l with respect to D^k and D^{k_l}, resp., $A_x^{k_l}$ and $A_y^{k_l}$ are the Jacobians in neighbor element D^{k_l}, and we have set $\Delta t = t^{n+1} - t^n$. See [8] for the precise derivation of Eqs. (10) and definition of matrices M^+ and M^-. On edges located on the computational boundary, $\partial\tilde{\Omega}$, we pose an outflow condition by setting $M^- = 0$.

Equations for $\tilde{q}^{n+1/2}$ can be obtained in a similar way. Multiplying both sides of the second system of PDEs in (6) with a test function ϕ^i, integrating over $\mathsf{D}^k \times (t^n; t^{n+1})$ (D^k in the PML region), and using (9) yield

$$\int_{\mathsf{D}^k} \phi^i \cdot \tilde{q}^{n+1/2} = \int_{\mathsf{D}^k} \phi^i \cdot \tilde{q}^n - \int_{\mathsf{D}^k} (\phi^i)^T \cdot A_x \cdot \sum_{j=0}^{N-1} \frac{\Delta t^{j+1}}{(j+1)!}\,[-A_x\,\partial_x - A_y\,\partial_y]^j\,\partial_x q^n \qquad (i = 1,\ldots,N_p)\,. \tag{11}$$

Notice that assembling the second integral on the right-hand side does not cause much extra work because the required products of A_x and A_y are already computed while assembling Eq. (10), and Eq. (11) has to be assembled only for elements in the PML region. Also notice that integrals in Eq. (11) containing spatial derivatives are not integrated by parts.

Step 2: Both initial value problems in Eqs. (7) can be solved analytically. Solving for $\tilde{q}$ first and then for q, we obtain

$$\tilde{q}^{n+2/3} = e^{-\sigma_1 \Delta t}\,\tilde{q}^{n+1/2}, \qquad q^{n+2/3} = e^{-\sigma_2 \Delta t}\,q^{n+1/2} + \left(e^{-\sigma_1 \Delta t} - e^{-\sigma_2 \Delta t}\right)\tilde{q}^{n+1/2}.$$

Step 3: The $(L^2(\mathsf{D}^k))^m$-norm of q_h can be computed directly from the degrees of freedom associated to D^k without using numerical quadrature. To see this, remember that $\{\phi^i\}$ is orthonormal in $(L^2(\mathsf{D}_R))^m$ and the grid elements D^k are straight-sided triangles. It holds

$$\int_{\mathsf{D}^k} |q_h(x,y,t)|^2\,dx\,dy = |J| \sum_{i,j=1}^{N_p} q_i^k(t)\,q_j^k(t) \int_{\mathsf{D}_R} \phi^i(\xi,\eta)\cdot\phi^j(\xi,\eta)\,d\xi\,d\eta = |J| \sum_{j=1}^{N_p} \left|q_j^k(t)\right|^2$$

where the Jacobian determinant, $J = \det\big(\partial(x,y)/\partial(\xi,\eta)\big)$, is constant in each element. Now, the computation of q^{n+1} and $\tilde{q}^{n+1}$ from relations (8) is straight-forward.

NUMERICAL EXAMPLES

We show two examples where the method presented above is applied to solve the acoustic wave equation (1) and (2). Material parameters in both examples are taken from [12]. The domain of interest is set to $\Omega = (-6,3)^2$, initial

conditions are pressure perturbations centered at the origin and a fourth order scheme is used. Damping functions are defined by $\sigma_1(x) = \bar{\sigma}\, d(x)$ and $\sigma_2(y) = \bar{\sigma}\, d(y)$ where $\bar{\sigma}$ is constant and $d(s) = \max\big(0, s-3, 6-s\big)$.

The first example considers a homogeneous medium with $\rho = 2.051$ and $E = 8.7036$ (in units $1\mathrm{e}{+12}\,\mathtt{kg}\cdot\mathtt{km}^{-3}$ and $1\mathrm{e}{+12}\,\mathtt{kg}\cdot\mathtt{km}^{-1}\cdot\mathtt{s}^{-2}$). The computational domain $\tilde{\Omega} = (-10.5, 7.5)^2$ is triangulated by about 15,000 triangles, and $\bar{\sigma} = 1$. Snapshots of the computed absolute pressure, $|p|$, are shown in Fig. 1. As can be seen, the amplitude of $|p|$ is damped in the PML region and the maximal value is reduced by about three orders of magnitude after $9\,s$ even though the method is not perfectly non-reflecting.

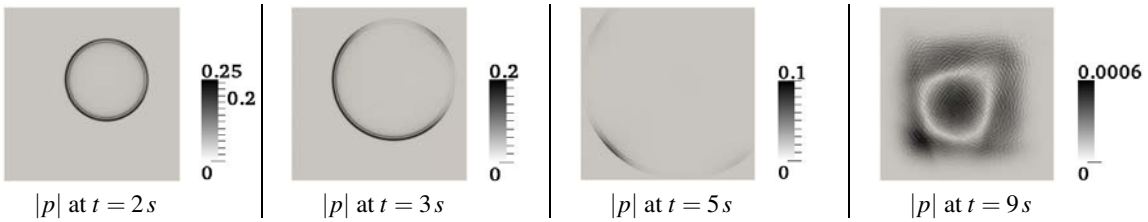

$|p|$ at $t = 2\,s$ | $|p|$ at $t = 3\,s$ | $|p|$ at $t = 5\,s$ | $|p|$ at $t = 9\,s$

FIGURE 1. Example 1: Snapshots of computed pressure field.

The second example considers a discontinuity in material parameters as depicted in the left image of Fig. 2. We use $\rho = 2.097$ and $E = 7.4116$ in the upper region (dark), and $\rho = 1.94$ and $E = 2.5656$ in the lower region (bright). The computational domain $\tilde{\Omega} = (-7.5, 4.5)^2$ is triangulated by about 11,000 triangles, and we set $\bar{\sigma} = 10$. In this case, the damping functions σ_1 and σ_2 show clear discontinuities when approximated by piecewise constant functions. Snapshots of the computed absolute pressure, $|p|$, are shown in Fig. 2. In this case, the stronger damping seems to generate stronger reflections at the PML interface. Nevertheless, the figures show that the proposed scheme yields reasonable damping of waves even if material parameters and damping functions are chosen discontinuous.

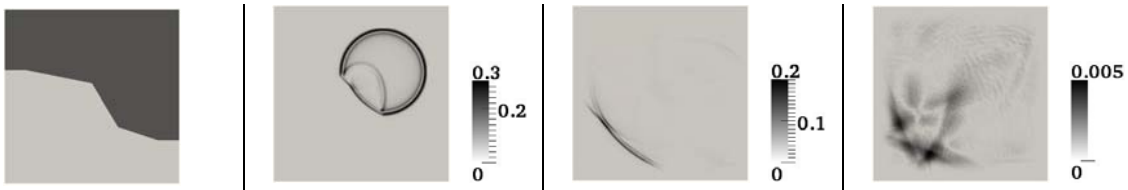

Distribution of materials | $|p|$ at $t = 1.5\,s$ | $|p|$ at $t = 5\,s$ | $|p|$ at $t = 9\,s$

FIGURE 2. Example 2: Distribution of materials and snapshots of computed pressure field.

REFERENCES

1. B. Engquist, and A. Majda, *Proceedings of the National Academy of Sciences* **74**, 1765–1766 (1977).
2. K. Duru, *Perfectly Matched Layers for Second Order Wave Equations*, Licentiate thesis, Department of Information Technology, Uppsala University (2010).
3. J.-L. Lions, J. Métral, and O. Vacus, *Numer. Math.* **92**, 535–562 (2002).
4. S. Abarbanel, D. Gottlieb, and J. S. Hesthaven, *J. Sci. Comput.* **17**, 405–422 (2002).
5. E. Bécache, S. Fauqueux, and P. Joly, Stability of Perfectly Matched Layers, Group Velocities and Anisotropic Waves, Rapport de recherche RR-4304, INRIA (2001).
6. D. Appelö, and G. Kreiss, *J. Comput. Phys.* **215**, 642–660 (2006).
7. R. L. LeVeque, *Finite Volume Methods for Hyperbolic Problems*, Cambridge University Press, Cambridge, 2002.
8. M. Käser, and M. Dumbser, *Geophysical Journal International* **166**, 855–877 (2006), ISSN 1365-246X.
9. J. S. Hesthaven, and T. Warburton, *Nodal Discontinuous Galerkin Methods*, vol. 54 of *Texts in Applied Mathematics*, Springer, New Yourk, 2008.
10. B. Rivière, *Discontinuous Galerkin Methods for Solving Elliptic and Parabolic Equations: Theory and Implementation*, Frontiers in Applied Mathematics, SIAM, Philadelphia, 2008.
11. M. Dumbser, and M. Käser, *Geophysical Journal International* **167**, 319–336 (2006).
12. J. Carcione, S. Picotti, D. Gei, and G. Rossi, *Pure and Applied Geophysics* **163**, 175–207 (2006).